Sādhanā (2020)45:171
https://doi.org/10.1007/s12046-020-01413-2

An analytical investigation of pressure-driven flow and heat transfer of a Sisko fluid flowing through parallel plates with viscous dissipation

SUMANTA CHAUDHURI[1] and SUSHIL KUMAR RATHORE[2,*]

[1]School of Mechanical Engineering, KIIT, Deemed to be University, Bhubanswar 751024, India
[2]Department of Mechanical Engineering, National Institute of Technology Rourkela, Rourkela 769008, India
e-mail: sc4692@gmail.com; isushilrathore@gmail.com

MS received 21 January 2020; revised 18 May 2020; accepted 11 June 2020

Abstract. Pressure driven flow of a Sisko fluid through rectangular parallel plates, having different wall temperatures is investigated considering the effect of viscous dissipation. The nonlinear momentum and energy conservation equations are solved employing homotopy perturbation method (HPM) and analytical solutions for the velocity, flow rate and temperature distributions are obtained. The analytical solution of pressure-driven flow and heat transfer characteristics of Sisko fluids flowing through parallel plates, taking into account viscous dissipation effect, has not been addressed earlier. For a special case of a typical Sisko fluid, the HPM solution exhibits an excellent agreement with the exact solution. Effects of various parameters such as Sisko fluid parameter, non-Newtonian index and Brinkman numbers on the variation of velocity and temperature are discussed. Further, temperature distribution in flow of Sisko fluids through parallel plates with both the plates maintained at same temperature is also obtained by a suitable substitution in the expression for temperature distribution. It is observed that the velocity decreases significantly with an increase in Sisko fluid parameter. Temperature of the fluid decreases with an increase in Sisko fluid parameter and displays an increasing trend with an increase in Brinkman number. Results of the present study are useful for designing thermal systems handling polymer flows. For the typical case of two plates having same temperature, the maximum temperature is observed to occur at the centre, which is attributed to the effect of viscous dissipation acting as an internal source. The theoretical framework developed and analytical solution provided for the problem under consideration may be taken as benchmark result for validation of future work.

Keywords. Sisko fluid; pressure-driven flow; homotopy perturbation method; homotopy analysis method; viscous dissipation.

1. Introduction

Flow of non-Newtonian fluids through different geometries has been an active area of research not only due to the challenge involved in its analysis, but also for its practical importance. Rheological behavior of a non-Newtonian fluid is too complicated to be described by a single constitutive equation. Therefore, several non-Newtonian fluid models have been proposed by the researchers which come under the broad category of shear thickening or dilatant fluids, shear thinning or pseudoplastic fluids, viscoplastic fluids, and viscoelastic fluids, etc. Power law model is a frequently applied non-Newtonian fluid model which describes the behavior of both shear thinning and shear thickening fluids. Sisko model is an extension of power law model which, too, can explain the flow behavior of shear thinning and shear thickening fluids. Lubricating oils used in the bearings, glues, various grades of protective and decorative paintings, etc. are some of the non-Newtonian fluids frequently used in engineering applications. Researchers [1–6] have investigated flow of various non-Newtonian fluids under diverse situations.

Sisko fluid model, put forward by Sisko [7], is one of the several non-Newtonian models. The Sisko constitutive equation involves three parameters which vary for different fluids. Sisko fluid model can be regarded as an extension of the power law model (a two parameter model) and this model can describe rheological behaviour of the fluids over a wide range of experimental data. If power law model is fitted over a wide range of experimental data, then for different ranges of data, the values of the constants will differ. Compared to this, Sisko model, being a three parameter model, can yield a better fit over a relatively wider range of data with single set of constants. However, this can not be generalized for all fluids. Lubricating oils, cement slurries, various paints, polymers, food products used in the food processing industry are observed to follow the Sisko fluid model (Khan and Shahzad [8], Khan *et al*

*For correspondence
Published online: 02 July 2020

[9]). A brief description about the previous studies on flow and heat transfer aspects of Sisko fluids is given below.

Belt-driven transport of a Sisko fluid has been studied by the researchers (Siddiqui *et al* [10]) and an analytical solution for the velocity has been obtained. The momentum conservation equation describing the flow is non-linear in nature and homotopy perturbation method, an analytical technique, has been employed to obtain the solution of the velocity. Effects of the non-Newtonian Sisko fluid parameter and non-Newtonian index on the velocity have been examined. Internal flow of Sisko fluid has drawn wide attention of the researchers and various cases, like Poiseuille flow, Coutte-Poiseuille flow and heat transfer have been investigated. Pressure-driven flow (Poiseuille flow) and heat transfer of a Sisko fluid, flowing through an annular pipe has been studied (Khan *et al* [9]). Non-linear governing differential equations have been solved by applying homotopy analysis method (HAM) and the effects of the non-Newtonian Sisko fluid parameter, viscous dissipation on the field variables have been analyzed and discussed. It has been observed that the non-Newtonian Sisko fluid parameter has similar effect on temperature as that of Brinkman number. Heat transfer effect for flow of a Sisko fluid over a stretching sheet has been investigated (Khan and Shahzad [11]). Partial differential equations, describing the physical phenomenon, have been reduced to non-linear ordinary differential equations by a suitable boundary layer approximation. The reduced equations have been solved employing HAM and the effect of various parameters on velocity and temperature have been studied. In few recent studies, Sisko constitutive equation has been employed to model the blood flow in peristalsis. Propagation of progressive waves through contraction and expansion of channel walls causing transportation of fluids is known as peristalsis. Peristaltic flows has diverge biological and industrial applications such as pumping of blood in heart, transportation of mordant fluids, lung machines. An interesting analytical study (Bhatti *et al* [12]) on peristaltic blood flow, modelling blood by Sisko constitutive equation, having magneto-nano particles has been carried out. The presence of magneto-nano particles in the blood results in a better control over the flow under the application of externally imposed magnetic field. The equations governing the flow and heat transfer problem are simplified based on the long wave length and low Reynold's number approximation, and the simplified equations have been solved by applying HPM. The effects of magnetic field, viscous dissipation, non-Newtonian parameter on the field variables are analyzed. In the previous study, the thermal conductivity has been assumed to be independent of temperature. This assumption, however, is not valid for large temperature difference. This shortcoming has been addressed by the researchers (Shaheen and Asjad [13]) considering peristaltic blood flow and heat transfer in the presence of externally imposed magnetic field, including the effect of variable thermal conductivity. Very recently, peristaltic motion of blood, including the heat transfer effect, in a porous medium has been investigated (Zeeshan *et al* [14]). Sisko constitutive equation is employed to model the blood flow in the arteries. Under the assumption of long wave length approximation, the PDEs are reduced to ODE and have been solved by an implicit finite difference scheme and the effects of various parameters on the flow and heat transfer have been analyzed. Researchers have addressed some advanced aspects of flow of Sisko fluid like the effect of Brownian motion and thermophoresis. Three-dimensional mixed convection flow of a Sisko fluid driven by stretched surface including the effects of Brownian motion and thermophoresis has been studied (Hayat *et al* [15]). Effects of the pertinent parameters on the velocity, temperature and concentration profile have been discussed. In all these previous studies, traditional methods of handling differential equations have been employed to find the solution. In a recent study, Artificial neural network (ANN) based statistical model has also been developed (Raja *et al* [16]) for analyzing the Sisko fluid dynamics (SFD).

In the preceding discussion, studies related to flow and heat transfer of Sisko fluid and their various aspects have been described. Effect of viscous dissipation has been considered in some of these studies, and is neglected in many. Thermal effect of the viscous dissipation, though neglected in many applications, is significant in typical situations as the quality of different products and the effectiveness of many lubricating systems are strongly temperature dependent. In such cases, it is essential to know the temperature distribution along with the flow field. Viscous dissipation can play a significant role in case of non-Newtonian fluids particularly in case of the pressure driven flow and flow driven by both pressure and shear force in polymer melt flow thorough channels and tubes. Thermal conductivity of the polymer is low and viscosity is high. Therefore, viscous dissipation is high in case of polymer processing and typical values of Brinkman number ranges from 0.1-10 (Gupta [17]). For example, in a study by the researchers (Khan *et al* [18]) of wire coating operation, Brinkman number has been varied in the range 1-4. Accordingly, effect of the viscous dissipation has to be considered in these cases and has been investigated by the researchers (Hayat *et al* [15], Khan *et al* [9], Shaheen and Asjad [13], Zeeshan *et al* [14].

The studies reported in the preceding discussion reveal that both basic aspects and advanced topics on Sisko fluids such as peristaltic flow, flow through porous media, magnetohydrodynamics (MHD), ANN modeling of Sisko fluids have been examined. But studies on basic aspects like flow and heat transfer through parallel plates subjected various boundary conditions, forced and mixed convection studies through cylindrical geometries for different boundary conditions can still be carried out for better understanding the physics of flow and heat transfer. In view of this, the present work considers pressure driven flow of a Sisko fluid

through rectangular parallel plates considering the effect of viscous dissipation. The system description involves nonlinear differential equations governing the flow and heat transfer. Though, over the years, different techniques have been evolved for solution of nonlinear differential equations including different numerical techniques, in general, such solutions are challenging. In comparison with numerical solutions, analytical or semi-analytical solutions often present a better physical insight into the physics of the problem as parametric dependence relation is expressed in the form of equations. It is therefore not surprising that there is a continuous endeavor to propose newer techniques for analytical solution of nonlinear differential equations. As a part of such effort, an elegant and powerful analytical technique HPM was introduced by He [19], He [20], He [21]). HPM is an infinite series solution technique which can take full advantage of the traditional perturbation method, but does not require the presence of any small or large parameter in the problem. It can be applied comparatively easily, but not at the cost of accuracy if the guess solution is properly chosen and the homotopy is constructed correctly. Due to these aforesaid advantages, HPM is still being used as powerful analytical tool by the researchers (Bhatti *et al* [12], Saheen and Asjad [13], Siddiqui *et al* [10]) for effective tackling of non-linear problems. Pressure driven flow of a Sisko fluid through annular pipe has been investigated earlier, but flow and heat transfer through rectangular parallel plates has never been reported. In the present study, flow and heat transfer characteristics of a Sisko fluid flowing through parallel plates is considered and analytical solutions for the velocity and temperature are generated. To the best of authors' knowledge, this would be the first analytical solution for the problem under consideration. In addition, the solution may be used by future researchers for the validation purpose. The understading of flow physics of the problem is also important from the fundamental fluid mechanics points of view. Furthermore, an exact solution for the special case of non-Newtonian index two is also obtained. Velocity, flow rate and temperature distribution are obtained as functions of the pertinent parameters and a comparison is drawn between the HPM results and those obtained from exact solution for the special case of the non-Newtonian index. Effects of various parameters on the velocity, flow rate, temperature have been discussed.

2. Model formulation

Figure 1 represents the schematic of pressure driven flow of a Sisko fluid through rectangular parallel plates. The reference frame is chosen as shown in figure 1. The flow is assumed to be steady, laminar, fully developed, incompressible and with constant properties. The gap between the plates h is assumed to be narrow and the plates are very large in lateral direction normal to the plane of the diagram. The two walls are maintained at different temperatures as shown in the figure 1. Velocity increases up to the centre line from the lower wall, reaches a maximum at the center and then again decreases. Therefore, the slope of the velocity is positive for the lower half and negative for the upper half. This distinction is required to take care of the modulus sign present in the constitutive equation of the Sisko fluid.

2.1 *Governing equations*

For the required field variables we have to solve mass, momentum and energy conservation equations. As steady, incompressible, laminar flow is studied, governing equations in their generalized forms are not presented to avoid complication. However, few important equations describing the characteristics of non-Newtonian fluids are presented. Cauchy's stress tensor for Sisko fluids is as follows:

$$R = -pI + \left[a + b\left(\sqrt{0.5tr\left(A_1^2\right)}\right)^{n-1}\right] \tag{1}$$

$$A_1 = L + L^T,\ L = \nabla\vec{V} \tag{2}$$

Where, R, p, I, a, b, n, A_1, L, V are Cauchy's stress tensor, static pressure, unit matrix, material parameters, non-Newtonian index, Rivlin-Erickson tensor, velocity gradient matrix and velocity vector respectively. Under the assumption of hydrodynamically fully developed flow, we seek a velocity field of the following form:

$$V = [u(y), 0, 0] \tag{3}$$

Where, y is the dimensional coordinate in the direction perpendicular to the axial direction and u is the axial velocity component in the direction of flow. Using the velocity given in Eq. (3), the momentum conservation equation for the problem addressed in the present study is as follows:

$$a\frac{d^2u}{dy^2} + nb\frac{d^2u}{dy^2}\left|\frac{du}{dy}\right|^{n-1} = \frac{dp}{dx} \tag{4}$$

Where, x is the dimensional axial coordinate. Using the form of velocity given by Eq. (3), the energy equation can be obtained as follows:

$$k\left(\frac{\partial^2 T}{\partial x^2} + \frac{\partial^2 T}{\partial y^2}\right) + a\left(\frac{du}{dy}\right)^2 + b\left(\frac{du}{dy}\right)^2\left|\frac{du}{dy}\right|^{n-1} = \rho c_p u\frac{\partial T}{\partial x} \tag{5}$$

Where, T is the dimensional temperature. From the equations above, it is clear that b=0 represents the case of Newtonian fluid and a = 0 represents the power law fluid equations.

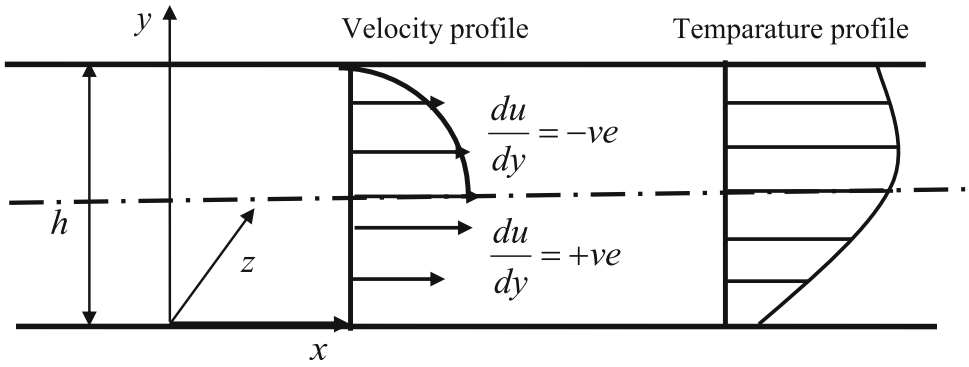

Figure 1. Schematic diagram of flow of Sisko fluid through rectangular parallel plates.

For non-dimensionalizing Eqs. (4) and (5), following non-dimensional variables are introduced

$$x^* = \frac{x}{l},\ y^* = \frac{y}{h},\ u^* = \frac{u}{u_0},\ p^* = \frac{p}{p_0},$$
$$\theta^* = \frac{T - T_b}{T_t - T_b}, N_1 = -\frac{dp}{dx}\frac{h^2}{au_0} \tag{6}$$

Where, x^*, y^*, u^*, p^*, θ^* are the non-dimensional coordinate in the axial and transverse direction, non-dimensional velocity, pressure, temperature respectively. h, l, u_0 are the gap between the parallel plates, length of the plates in the axial direction, and the reference velocity. A specific value of N_1 presents u_0 as the average velocity, but other values of N_1 signifies higher or lower values than the average velocity. T_b, $T_t$are the temperatures of the lower and upper walls respectively. Substituting the non-dimensional variables from Eq. (6) to Eq. (5), the non-dimensional momentum conservation equations is obtained as follows:

$$\frac{d^2u^*}{dy^{*2}} + nb^*\frac{d^2u^*}{dy^{*2}}\left|\frac{du^*}{dy^*}\right|^{n-1} = N_1 \tag{7}$$

On the basis of assumption of small gap between the plates, few terms in the energy equation can be discarded. The first term present in Eq. (5), represents the axial conduction which is very small compared to the conduction in the transverse direction as the length scale along y direction is very small compared to the length scale in the x direction. Further, the term in the right hand side of Eq. (5) representing the convection effect can be neglected. The energy conservation equation in its non-dimensional form is as follows.

$$\frac{\partial^2\theta^*}{\partial y^{*2}} + \mathrm{Br}\left(\frac{du^*}{dy^*}\right)^2 + \mathrm{Br}b^*\left(\frac{du^*}{dy^*}\right)^2\left|\frac{du^*}{dy^*}\right|^{n-1} = \mathrm{Pe}\left(\frac{h}{l}\right)\frac{\partial\theta^*}{\partial x^*} \tag{8}$$

We also define the following non-dimensional parameters:

$$\mathrm{Ec} = \frac{u_0^2}{c_p(T_t - T_b)}, \mathrm{Pr} = \frac{ac_p}{k}, \mathrm{Br} = \mathrm{Pr}\,\mathrm{Ec},$$
$$b^* = \frac{b}{a\left(\frac{h}{u_0}\right)^{n-1}}, \mathrm{Pe} = \frac{\rho c_p u_0 h}{k} \tag{9}$$

Where, Ec, Pr, Br, Pe, b^* are the Eckert number, Prandtl number, Brinkman number, Peclet number, and Sisko fluid parameter respectively. For low density polymer (LDPE) typical value of density (ρ) is 910 kg/m^3 [17] specific heat (c_p) is 1900 J/kg.k [17], thermal conductivity is 0.30 W/m.K [17]. Order of the average velocity can be considered to vary from 0.001 to 0.01 m/s [17] and the order of the gap between the plates can vary from 0.001 to 0.01 m [17]. With these values, Peclet number ranges from 10 to 1000. However, from Eq. (8) it is evident that the presence of the term h/l (0.01-0.1) with Peclet number diminishes its effect (thus making the net effect of the Peclet number to be little) and the contribution of the convective term turns out to be marginal. If smallest value of the Peclet number 10 is considered and h/l is considered to be 0.01, then Pe h/l is coming to be 0.1. However, for other values of Peclet number, and h/l, the assumption of negligible convective heat transfer is not valid. The assumption is only valid for a very small gap between the plates. This factor implies that heat transfer is dominated by conduction and convective heat transfer along axial direction can be neglected. Therefore, temperature reduces to a function of y only. As a result, Eq. (8) reduces to the following:

$$\frac{d^2\theta^*}{dy^{*2}} + \mathrm{Br}\left(\frac{du^*}{dy^*}\right)^2 + \mathrm{Br}b^*\left(\frac{du^*}{dy^*}\right)^2\left|\frac{du^*}{dy^*}\right|^{n-1} = 0 \tag{10}$$

As the velocity distribution is symmetric about the centre, velocity decreases with increase in y in the upward direction from the centre line as shown in figure 1. Therefore, $\frac{du^*}{dy^*}$ is negative which gives $\left|\frac{du^*}{dy^*}\right| = -\frac{du^*}{dy^*}$ and to take this change in sign into account, it is essential to write the equations for the lower and upper parts separately.

2.2 *Equations taking modulus sign into account*

Momentum and energy conservation equations for the lower half are given as follows:

$$\frac{d^2u_1^*}{dy^{*2}} + nb^* \frac{d^2u_1^*}{dy^{*2}} \left(\frac{du_1^*}{dy^*}\right)^{n-1} = N_1 \tag{11}$$

$$\frac{d^2\theta_1^*}{dy^{*2}} + \mathrm{Br}\left(\frac{du_1^*}{dy^*}\right)^2 + \mathrm{Br}b^* \left(\frac{du_1^*}{dy^*}\right)^2 \left(\frac{du_1^*}{dy^*}\right)^{n-1} = 0 \quad \text{for} \quad 0 \le y^* \le \frac{1}{2} \tag{12}$$

For the upper half, equations will be modified as given below:

$$\frac{d^2u_2^*}{dy^{*2}} + (-1)^{n-1} nb^* \frac{d^2u_2^*}{dy^{*2}} \left(\frac{du_2^*}{dy^*}\right)^{n-1} = N_1 \tag{13}$$

$$\frac{d^2\theta_2^*}{dy^{*2}} + \mathrm{Br}\left(\frac{du_2^*}{dy^*}\right)^2 + (-1)^{n-1}\mathrm{Br}b^* \left(\frac{du_2^*}{dy^*}\right)^2 \left(\frac{du_2^*}{dy^*}\right)^{n-1} = 0 \quad \text{for} \quad \frac{1}{2} \le y^* \le 1 \tag{14}$$

Where, u_1, u_2 and θ_1, θ_2 are velocity and temperature in lower and upper half, respectively.

2.3 *Non-dimensional boundary conditions*

For applying boundary conditions, expression of the shear stress for Sisko fluid is required, which is different from the Newtonian fluid as the constitutive equations are not the same. Therefore, at this point, it is essential to mention the equation of the shear stress for Sisko fluid which is given as below:

$$\tau = a\frac{du}{dy} + b\left(\left|\frac{du}{dy}\right|\right)^n \tag{15}$$

This equation will be useful again in the results and discussion part for detailed explanation and in this regard, the effective viscosity from Eq. (19) can be defined as follows:

$$\mu_{eff} = a + b\left(\left|\frac{du}{dy}\right|\right)^{n-1} \tag{16}$$

Non-dimensional shear stress equation is given below as:

$$\frac{\tau^*}{\tau_0} = \frac{du^*}{dy^*} + b^*\left(\frac{du^*}{dy^*}\right)^n \tag{17}$$

Where, the scale for shear stress

$$\tau_0 = \frac{au_0}{h} \tag{18}$$

Boundary conditions are given as follows:

$$\text{At, } y^* = 0,\ u_1^* = 0,\ \theta_1^* = 0 \tag{19.1}$$

(No slip and no temperature jump)

$$y^* = \frac{1}{2},\ u_1^* = u_2^*,\ \theta_1^* = \theta_2^* \tag{19.2}$$

(Continuity of velocity and temperature)

$$y^* = \frac{1}{2},\ \frac{du_1^*}{dy^*} = \frac{du_2^*}{dy^*},\ \frac{d\theta_1^*}{dy^*} = \frac{d\theta_2^*}{dy^*} \tag{19.3}$$

(Continuity of velocity gradient and temperature gradient)

$$y^* = 1,\ u_2^* = 0,\ \theta_2^* = 1 \tag{19.4}$$

(No slip and no temperature jump)

3. Implementation of HPM

Governing equations given in Eqs. (11) - Eq. (14) are uncoupled, but highly non-linear in nature. It is a formidable task to obtain an exact solution to these equations. For generating analytical solution, HPM is applied. The infinite series solution adopted in HPM has been observed to give convergent results in many cases for all practical purposes. However, like all other methods, HPM has its own limitations too. If the initial guess solution is not chosen properly, truncating the infinite series only up to 2nd or 3rd order can produce inaccurate results. Therefore, choosing the initial guess is very important in this method. Further, construction of the proper homotopy is also very crucial, failing which the results generated, may be divergent. For further details, one may refer to the literatures [Bhatti *et al* [12]; He [18]; He [19]; He [20]; Shaheen and Asjad [13]. For solving Eq. (11) and Eq. (13), following homotopy is constructed,

$$(1-q)\left[\frac{d^2v_1^*}{dy^{*2}} - \frac{d^2u_{10}^*}{dy^{*2}}\right] + q\left[\frac{d^2v_1^*}{dy^{*2}} + nb^*\frac{d^2v_1^*}{dy^{*2}}\left(\frac{dv_1^*}{dy^*}\right)^{n-1} - N_1\right] = 0 \tag{20}$$

$$(1-q)\left[\frac{d^2v_2^*}{dy^{*2}} - \frac{d^2u_{20}^*}{dy^{*2}}\right] + q\left[\frac{d^2v_2^*}{dy^{*2}} + (-1)^{n-1}nb^*\frac{d^2v_2^*}{dy^{*2}}\left(\frac{dv_2^*}{dy^*}\right)^{n-1} - N_1\right] = 0 \tag{21}$$

Where, q is an embedding parameter, u_{10}^*, u_{20}^* are initial guess solutions for u_1^*, u_2^* v_1^* and v_2^* are assumed to be the approximate solutions for u_1^* and u_2^* and are expanded in series up to the 2nd order as follows:

$$v_1^* = v_{10}^* + qv_{11}^* + q^2 v_{12}^* \tag{22.1}$$

$$v_2^* = v_{20}^* + qv_{21}^* + q^2 v_{22}^* \tag{22.2}$$

For obtaining the temperature field, expression for the velocity and temperature in the series form are substituted in the energy equations and coefficients of like powers of q are equated to get the equations of various orders.

Substituting Eq. (22.1) and Eq. (22.2) in Eq. (20) and Eq. (21) and equating the power of q^0, q^1, q^2 we get the governing equations for velocity for the 0th order, 1st order and 2nd order systems.

ϕ_1 and ϕ_2 are assumed to be the approximate series solution for non-dimensional temperatures θ_1 and θ_2 respectively and are expanded up to the 2nd order as follows:

$$\phi_1^* = \phi_{10}^* + q\phi_{11}^* + q^2\phi_{12}^* \tag{23.1}$$

$$\phi_2^* = \phi_{20}^* + q\phi_{21}^* + q^2\phi_{22}^* \tag{23.2}$$

Substituting Eq. (23.1) and Eq. (23.2) in Eq. (12) and Eq. (14), and equating the coefficients of q^0, q^1 and q^2 we get the 0th order, 1st order and 2nd order equation for temperature. For velocity and temperature the equation are given as follows:

3.1 *0th order system*

Equations for the 0th order system are as follows:

$$\frac{d^2 v_{10}^*}{dy^{*2}} - \frac{d^2 u_{10}^*}{dy^{*2}} = 0 \tag{24}$$

$$\frac{d^2\phi_{10}^*}{dy^{*2}} = -\mathrm{Br}\left(\frac{dv_{10}^*}{dy^*}\right)^2 - \mathrm{Br}b^*\left(\frac{dv_{10}^*}{dy^*}\right)^{n+1} \quad \text{for} \quad 0 \le y^* \le \frac{1}{2} \tag{25}$$

$$\frac{d^2 v_{20}^*}{dy^{*2}} - \frac{d^2 u_{20}^*}{dy^{*2}} = 0 \tag{26}$$

$$\frac{d^2\phi_{20}^*}{dy^{*2}} = -\mathrm{Br}\left(\frac{dv_{20}^*}{dy^*}\right)^2 - (-1)^{n-1}\mathrm{Br}b^*\left(\frac{dv_{20}^*}{dy^*}\right)^{n+1} \quad \text{for} \quad \frac{1}{2} \le y^* \le 1 \tag{27}$$

v_{10}^*, v_{20}^* and ϕ_{10}^*, ϕ_{20}^* are the 0th order solution for the velocity and the temperature in the lower and upper half respectively.

Boundary condition:

$$\text{At, } y^* = 0,\ v_{10}^* = 0,\ \phi_{10}^* = 0 \tag{28.1}$$

$$y^* = \frac{1}{2},\ v_{10}^* = v_{20}^*,\ \frac{dv_{10}^*}{dy^*} = \frac{dv_{20}^*}{dy^*},\ \phi_{10}^* = \phi_{20}^*,\ \frac{d\phi_{10}^*}{dy^*} = \frac{d\phi_{20}^*}{dy^*} \tag{28.2}$$

$$y^* = 1,\ v_{20}^* = 0,\ \phi_{20}^* = 1 \tag{28.3}$$

3.2 *1st order equations*

Equating the coefficients of q from Eq. (20), Eq. (21), Eq. (12), Eq. (14) following equations for the 1st order system are obtained:

$$\frac{d^2 v_{11}^*}{dy^{*2}} + \frac{d^2 u_{10}^*}{dy^{*2}} - N_1 + nb^*\frac{d^2 v_{10}^*}{dy^{*2}}\left(\frac{dv_{10}^*}{dy^*}\right)^{n-1} = 0 \tag{29.1}$$

$$\frac{d^2\phi_{11}^*}{dy^{*2}} + 2\mathrm{Br}\frac{dv_{10}^*}{dy^*}\frac{dv_{11}^*}{dy^*} + (n+1)\mathrm{Br}\left(\frac{dv_{10}^*}{dy^*}\right)^n\frac{dv_{11}^*}{dy^*} = 0 \quad \text{for} \quad 0 \le y^* \le \frac{1}{2} \tag{29.2}$$

$$\frac{d^2 v_{21}^*}{dy^{*2}} + \frac{d^2 u_{20}^*}{dy^{82}} - N_1 + (-1)^{n-1}nb^*\frac{d^2 v_{20}^*}{dy^{*2}}\left(\frac{dv_{20}^*}{dy^*}\right)^{n-1} = 0 \tag{29.3}$$

$$\frac{d^2\phi_{21}^*}{dy^{*2}} + 2\mathrm{Br}\frac{dv_{20}^*}{dy^*}\frac{dv_{21}^*}{dy^*} + (-1)^{n-1}(n+1)\mathrm{Br}b^*\left(\frac{dv_{20}^*}{dy^*}\right)^n\frac{dv_{21}^*}{dy^*} = 0 \quad \text{for} \quad \frac{1}{2} \le y^* \le 1 \tag{29.4}$$

v_{11}^*, v_{21}^* and ϕ_{11}*, ϕ_{21}* are the 1st order solution for the velocity and the temperature in the lower and upper half respectively.

Boundary conditions:

$$\text{At, } y^* = 0,\ v_{11}^* = 0,\ \phi_{11}^* = 0 \tag{30.1}$$

$$y^* = \frac{1}{2},\ v_{11}^* = v_{21}^*,\ \frac{dv_{11}^*}{dy^*} = \frac{dv_{21}^*}{dy^*},\ \phi_{11}^* = \phi_{21}^*,\ \frac{d\phi_{11}^*}{dy^*} = \frac{d\phi_{21}^*}{dy^*} \tag{30.2}$$

$$y^* = 1,\ v_{21}^* = 0,\ \phi_{21}^* = 1 \tag{30.3}$$

3.3 *2nd order equations*

Equating the coefficients of q^2 to zero from Eq. (20), Eq. (21), Eq. (12) and Eq. (14) equations for the 2nd order system are found as follows:

$$\frac{d^2v_{12}^*}{dy^{*2}} + n(n-1)b^*\frac{d^2v_{20}^*}{dy^{*2}}\left(\frac{dv_{20}^*}{dy^*}\right)^{n-2}\frac{dv_{11}^*}{dy^*} + nb^*\frac{d^2v_{11}^*}{dy^{*2}}\left(\frac{dv_{10}^*}{dy^*}\right)^{n-1} = 0 \tag{31.1}$$

$$\frac{d^2\phi_{12}^*}{dy^{*2}} + \mathrm{Br}\left(\frac{dv_{11}^*}{dy^*}\right)^2 + 2\mathrm{Br}\frac{dv_{10}^*}{dy^*}\frac{dv_{12}^*}{dy^*} + (n+1)\mathrm{Br}b^*\left(\frac{dv_{10}^*}{dy^*}\right)^n\frac{dv_{12}^*}{dy^*} + \frac{n(n+1)}{2}\mathrm{Br}b^*\left(\frac{dv_{10}^*}{dy^*}\right)^{n-1}\left(\frac{dv_{11}^*}{dy^*}\right)^2 = 0 \quad \text{for} \quad \frac{1}{2} \le y^* \le \frac{1}{2} \tag{31.2}$$

$$\frac{d^2v_{22}^*}{dy^{*2}} + (-1)^{n-1}n(n-1)b^*\frac{d^2v_{20}^*}{dy^{*2}}\left(\frac{dv_{20}^*}{dy^*}\right)^{n-2}\frac{dv_{21}^*}{dy^*} + (-1)^{n-1}nb^*\frac{d^2v_{21}^*}{dy^{*2}}\left(\frac{dv_{10}^*}{dy^*}\right)^{n-1} = 0 \tag{31.3}$$

$$\frac{d^2\phi_{22}^*}{dy^{*2}} + \mathrm{Br}\left(\frac{dv_{21}^*}{dy^*}\right)^2 + 2\mathrm{Br}\frac{dv_{20}^*}{dy^*}\frac{dv_{22}^*}{dy^*} + (-1)^{n-1}(n+1)\mathrm{Br}b^*\left(\frac{dv_{20}^*}{dy^*}\right)^n\frac{dv_{22}^*}{dy^*} + (-1)^{n-1}\frac{n(n+1)}{2}\mathrm{Br}b^*\left(\frac{dv_{20}^*}{dy^*}\right)^n\left(\frac{dv_{21}^*}{dy^*}\right)^2 = 0 \quad \text{for} \quad \frac{1}{2} \le y^* \le 1 \tag{31.4}$$

v_{12}, v_{22} and ϕ_{12}, ϕ_{22} are the 2nd order solution for the velocity and the temperature in the lower and upper half respectively.

Boundary conditions:

$$\text{At, } y^* = 0,\ v_{12} = 0,\ \phi_{12} = 0 \tag{32.1}$$

$$y^* = \frac{1}{2},\ v_{12}^* = v_{22}^*,\ \frac{dv_{12}^*}{dy^*} = \frac{dv_{22}^*}{dy^*},\ \phi_{12}^* = \phi_{22}^*,\ \frac{d\phi_{12}^*}{dy^*} = \frac{d\phi_{22}^*}{dy^*} \tag{32.2}$$

$$y^* = 1,\ v_{22}^* = 0,\ \phi_{22}^* = 1 \tag{32.3}$$

4. Solution by HPM

4.1 *Solution for 0th order equation*

Selection of a guess solution is a very crucial task in the success of HPM. If it is properly chosen, then even if the series is truncated after few terms, the results generated are within a reasonable accuracy for a wide range of the parameters involved in the problem. A little change in the guess solution may increase the range of parameters of the convergence or the rate of convergence to a large extent. In the present problem, for selecting the guess solution, we have put n=1in Eq. (11). By doing so, we expect that we have started with the solution which satisfies the equation for n=1 and for other n, including more terms of the 1st and 2nd order solution we can march close to the actual solution. Thus we chose the guess solution as follows:

$$u_{10}^* = u_{20}^* = \frac{N_1}{2(1+b^*)}(y^{*2} - y^*) \tag{33.1}$$

Substituting u_{10} and u_{20} in Eqs. (24) and Eq. (26) and using the boundary conditions given in Eqs. (28.1-28.3) v_{10}^* and v_{20}^* are obtained to be same as u_{10}^* and u_{20}^*. Substituting v_{10} and v_{20} in Eqs. (25) and Eq. (27) ϕ_{10}^* and ϕ_{20}^* are solved. The equations are given as follows:

$$u_{10}^* = u_{20}^* = v_{10}^* = v_{20}^* \tag{33.2}$$

$$\phi_{10}^* = y^* + \frac{\mathrm{Br}N_1^2\left(\frac{y^*}{6} - \frac{y^{*4}}{3} + \frac{2y^{*3}}{3} - \frac{y^{*2}}{2}\right)}{4(1+b^*)^2} + \frac{\mathrm{Br}b^*N_1^{n+1}\left[(-1)^{n+3} - (2y^*-1)^{n+3}\right]}{2^{n+3}(1+b^*)^{n+1}(n+2)(n+3)} \quad \text{for} \quad 0 \le y^* \le \frac{1}{2} \tag{33.3}$$

$$\phi_{20}^* = y^* + \frac{\mathrm{Br}N_1^2\left(\frac{y^*}{6} - \frac{y^{*4}}{3} + \frac{2y^{*3}}{3} - \frac{y^{*2}}{2}\right)}{4(1+b^*)^2} + \frac{\mathrm{Br}b^*N_1^{n+1}\left[(-1)^{n+3} - (-1)^{n-1}(2y^*-1)^{n+3}\right]}{2^{n+3}(1+b^*)^{n+1}(n+2)(n+3)} \quad \text{for} \quad \frac{1}{2} \le y^* \le 1 \tag{33.4}$$

4.2 *Solution for 1st order equation*

The 1st order solution is obtained by substituting Eqs. (33.1)- Eq.(33.2) in Eqs. (29.1)- Eq. (29.4) and solving for the velocity and temperature satisfying the boundary conditions given by Eqs. (30.1)-Eq. (30.3). The solutions obtained are as follows:

$$v_{11}^* = \frac{N_1b^*(y^{*2} - y^*)}{2(1+b^*)} + \frac{b^*N_1^n\left[(-1)^{n+1} - (2y^*-1)^{n+1}\right]}{2^{n+1}(n+1)(1+b^*)^n} \tag{34.1}$$

$$v_{21}^{*}=\frac{N_1 b^{*}(y^{*2}-y^{*})}{2(1+b^{*})}+\frac{b^{*}N_1^{n}\left[(-1)^{n+1}-(-1)^{n-1}(2y^{*}-1)^{n+1}\right]}{2^{n+1}(n+1)(1+b^{*})^{n}} \tag{34.2}$$

$$\begin{aligned}\phi_{11}^{*}&=\mathrm{Br}N_1^{2}b^{*}(\frac{y^{*}}{6}-\frac{y^{*4}}{3}+\frac{2y^{*3}}{3}-\frac{y^{*2}}{2})\\&+\frac{\mathrm{Br}b^{*}N_1^{n+1}\{1-0.5(n+1)\}[(2y^{*}-1)^{n+3}-(-1)^{n+3}]}{(1+b^{*})^{n+1}(n+2)(n+3)2^{n+2}}\\&+\frac{\mathrm{Br}b^{*}N_1^{2n}(n+1)\left[(2y^{*}-1)^{2n+2}-1\right]}{2^{2n+2}(1+b^{*})^{2n}(2n+1)(2n+2)}\\&\text{for}\quad 0\le y^{*}\le\frac{1}{2}\end{aligned} \tag{34.3}$$

$$\begin{aligned}\phi_{21}^{*}&=\frac{\mathrm{Br}N_1^{2}b^{*}(\frac{y^{*}}{6}-\frac{y^{*4}}{3}+\frac{2y^{*3}}{3}-\frac{y^{*2}}{2})}{2(1+b)^{2}}\\&+\frac{\mathrm{Br}b^{*}N_1^{n+1}\left\{1-\frac{(n+1)b^{*}}{2}\right\}\left[-1+(-1)^{n+3}(2y^{*}-1)^{n+3}\right]}{2^{n+2}(1+b^{*})^{n+1}(n+2)(n+3)}\\&+\frac{\mathrm{Br}b^{*2}N_1^{2n}(n+1)\left[(2y^{*}-1)^{2n+2}-1\right]}{2^{2n+2}(1+b^{*})^{2n}(2n+1)(2n+2)}\\&\text{for}\quad\frac{1}{2}\le y^{*}\le 1\end{aligned} \tag{34.4}$$

4.3 *Solution for 2nd order equation*

Equtaions (31.1) and (31.4) along with the boundary conditions of Eqs. (32.1)-Eq.(32.3) are solved by substituting Eqs. (34.1)-Eq.(34.2) in these. The following solutions are obtained:

$$v_{12}^{*}=\frac{nb^{*2}N_1^{n}\left[(-1)^{n+1}-(2y^{*}-1)^{n+1}\right]}{2^{n+1}(n+1)(1+b^{*})^{n}}+\frac{b^{*2}N_1^{2n-1}\left[(2y^{*}-1)^{2n}-1\right]}{2^{2n+1}(1+b^{*})^{2n-1}} \tag{35.1}$$

$$v_{22}^{*}=\frac{nb^{*2}N_1^{n}\left[(-1)^{n+1}-(-1)^{n-1}(2y^{*}-1)^{n+1}\right]}{2^{n+1}(n+1)(1+b^{*})^{n}}+\frac{b^{*2}N_1^{2n-1}\left[(2y^{*}-1)^{2n}-1\right]}{2^{2n+1}(1+b^{*})^{2n-1}} \tag{35.2}$$

$$\begin{aligned}\phi_{12}^{*}&=\left[\begin{array}{l}\frac{\mathrm{Br}N_1^{2}b^{*2}}{4(1+b^{*})^{2}}(\frac{y^{*}}{6}-\frac{y^{*4}}{3}+\frac{2y^{*3}}{3}-\frac{y^{*2}}{2})\\+\frac{\mathrm{Br}b^{*2}N_1^{2n}\left\{1-(2y^{*}-1)^{2n+2}\right\}}{2^{2n+2}(1+b^{*})^{2n}(2n+1)(2n+2)}\\+\frac{\mathrm{Br}N_1^{n+1}b^{*2}\left\{-(2y^{*}-1)^{n+3}+(-1)^{n+3}\right\}}{2^{n+2}(1+b^{*})^{n+1}(n+2)(n+3)}\end{array}\right]\\&+\left[\begin{array}{l}\frac{\mathrm{Br}nb^{*2}N_1^{n+1}\left\{(2y^{*}-1)^{n+3}-(-1)^{n+3}\right\}}{2^{n+2}(1+b^{*})^{n+1}(n+2)(n+3)}\\+\frac{n\mathrm{Br}N_1^{2n}b^{*2}\left\{1-(2y^{*}-1)^{2n+2}\right\}}{2^{2n+1}(1+b^{*})^{2n}(2n+1)(2n+2)}\end{array}\right]\\&+\left[\begin{array}{l}\frac{n(n+1)\mathrm{Br}b^{*3}N_1^{2n}\left\{(2y^{*}-1)^{2n+2}-1\right\}}{2^{2n+2}(1+b^{*})^{2n}(2n+1)(2n+2)}\\+\frac{n(n+1)\mathrm{Br}N_1^{3n-1}b^{*3}\left\{-(2y^{*}-1)^{3n+1}+(-1)^{3n+1}\right\}}{2^{3n+1}(1+b^{*})^{3n-1}3n(3n+1)}\end{array}\right]\\&\frac{n(n+1)\mathrm{Br}b^{*3}N_1^{2n}[(2y^{*}-1)^{2n+2}-1]}{2^{2n+2}(1+b^{*})^{2n}(2n+1)(2n+2)}\\&+\frac{n(n+1)\mathrm{Br}b^{*3}N_1^{n+1}[(-1)^{n+3}-(2y^{*}-1)^{n+3}]}{2^{n+4}(1+b)^{n+1}(n+2)(n+3)}\\&+\frac{n(n+1)\mathrm{Br}b^{*3}N_1^{3n-1}\left\{-(2y^{*}-1)^{3n+1}+(-1)^{3n+1}\right\}}{2^{3n+2}(1+b^{*})^{3n-1}3n(3n+1)}\\&0\le y^{*}\le\frac{1}{2}\end{aligned} \tag{35.3}$$

$$\begin{aligned}\phi_{22}^{*}&=\left[\begin{array}{l}\frac{\mathrm{Br}N_1^{2}b^{*2}}{4(1+b^{*})^{2}}(\frac{y^{*}}{6}-\frac{y^{*4}}{3}+\frac{2y^{*3}}{3}-\frac{y^{*2}}{2})\\-\frac{\mathrm{Br}b^{*2}N_1^{2n}\left\{(2y^{*}-1)^{2n+2}-1\right\}}{2^{2n+2}(1+b^{*})^{2n}(2n+1)(2n+2)}\\+\frac{\mathrm{Br}N_1^{n+1}b^{*2}\left\{(-1)^{n-1}(2y^{*}-1)^{n+3}-(-1)^{n+3}\right\}}{2^{n+2}(1+b^{*})^{n+1}(n+2)(n+3)}\end{array}\right]\\&+\left[\begin{array}{l}\frac{n\mathrm{Br}b^{*2}N_1^{n+1}\left\{(-1)^{n-1}(2y^{*}-1)^{n+3}-(-1)^{n+3}\right\}}{2^{n+2}(1+b^{*})^{n+1}(n+2)(n+3)}\\-\frac{n\mathrm{Br}N_1^{2n}b^{*2}\left\{(2y^{*}-1)^{2n+2}-1\right\}}{2^{2n+2}(1+b^{*})^{2n}(2n+1)(2n+2)}\end{array}\right]\\&+\left[\begin{array}{l}\frac{n(n+1)\mathrm{Br}b^{*3}N_1^{2n}\left\{(2y^{*}-1)^{2n+2}-1\right\}}{2^{2n+2}(1+b^{*})^{2n}(2n+1)(2n+2)}\\+\frac{n(n+1)\mathrm{Br}N_1^{3n-1}b^{*3}\left\{-(-1)^{n-1}(2y^{*}-1)^{3n+1}+(-1)^{3n+1}\right\}}{2^{3n+1}(1+b^{*})^{3n-1}3n(3n+1)}\end{array}\right]\\&\frac{n(n+1)\mathrm{Br}b^{*3}N_1^{2n}[(2y^{*}-1)^{2n+2}-1]}{2^{2n+2}(1+b^{*})^{2n}(2n+1)(2n+2)}\\&+\frac{n(n+1)\mathrm{Br}b^{*3}N_1^{n+1}[(-1)^{n+3}-(-1)^{n-1}(2y^{*}-1)^{n+3}]}{2^{n+4}(1+b)^{n+1}(n+2)(n+3)}\\&+\frac{n(n+1)\mathrm{Br}b^{*3}N_1^{3n-1}\left\{-(-1)^{n-1}(2y^{*}-1)^{3n+1}+(-1)^{3n+1}\right\}}{2^{3n+2}(1+b^{*})^{3n-1}3n(3n+1)}\end{aligned} \tag{35.4}$$

Now, according to HPM, we have to put q =1 in Eq. (22.1)-Eq. (22.2) and Eq. (23.1)-Eq. (23.2) for generating analytical solution for the velocity and temperature field as given below:

$$u_1^* = v_1^* = v_{10}^* + v_{11}^* + v_{12}^* \tag{36.1}$$

$$u_2^* = v_2^* = v_{20}^* + v_{21}^* + v_{22}^* \tag{36.2}$$

$$\phi_1^* = \phi_{10}^* + \phi_{11}^* + \phi_{12}^* \tag{36.3}$$

$$\phi_2^* = \phi_{20}^* + \phi_{21}^* + \phi_{22}^* \tag{36.4}$$

4.4 *Flow rate*

Expressions for the non-dimensional flow rate are obtained by integrating velocity with respect to y over the entire domain, which is as follows:

$$\begin{aligned} Q^* = &-\frac{N_1}{12} + \frac{b^* N_1^n (1+nb^*)}{2^{n+2}(1+b^*)^n (n+1)}\left[(-1)^{n+1} + \frac{(-1)^{n+2}}{n+2}\right] \\ &- \frac{b^{*2} N_1^{2n-1}}{2^{2n+2}(1+b^*)^{2n-1}}\left[\frac{(-1)^{2n+1}}{2n+1} + 1\right] \\ &+ \frac{b^* N_1^n (1+nb^*)}{2^{n+2}(1+b^*)^n (n+1)}[(-1)^{n+1} \\ &- \frac{(-1)^{n-2}}{(n+2)}] + \frac{b^{*2} N_1^{2n-1}}{2^{2n+2}(1+b^*)^{2n-1}}\left[\frac{1}{2n+1} - 1\right] \end{aligned} \tag{37}$$

Where, Q^* is the dimensionless flow rate given as

$$Q^* = \frac{\hat{Q}_f}{u_0 h} \tag{38}$$

$\hat{Q}_f$ is dimensional flow rate. A special case is discussed when both the walls are at the same temperature. It can be shown that for this case, the solution for the temperature is obtained from Eq. (23.1) and Eq. (23.2) by equating the 1st term (y) to zero.

5. Exact solution

For validation, a closed form analytical solution is obtained for non-Newtonian index 2. For other values of non-Newtonian index n=3 and 4, closed form analytical solution may not be admissible, or even if it exists, it is a formidable task to get these solution. Therefore, in the present study, closed form analytical solution or exact solution is attempted only for n=2. For n = 2, an exact solution is obtained for Eqs. (11)–(14) along with the boundary conditions Eqs. (19.1)–Eq. (19.3). Equation (11) can be solved by simple substitution for velocity gradient and then solving for u_1^*. Similarly, the solution for u_2^* can also be obtained. Then θ_1^* and θ_2^* can be solved. The solutions are as follows:

$$u_1^* = \frac{1}{2b}\left[-y^* + \frac{\{1+4b^*(N_1 y^* + c_1)\}^{\frac{3}{2}}}{6b^* N_1}\right] + c_2 \tag{39.1}$$

$$u_2^* = \frac{1}{2b^*}\left[y^* + \frac{\{1-4b^*(N_1 y^* + c_3\}^{\frac{3}{2}}}{6b^* N_1}\right] + c_4 \tag{39.2}$$

$$\begin{aligned} \theta_1^* = &-\frac{\mathrm{Br}}{4b^{*2}}\left[y^{*2} + 2b^* N_1 \frac{y^3}{3} + 2b^* c_1 y^{*2} \right. \\ &\left. - \frac{\{1+4b(N_1 y^* + c_1)\}^{\frac{3}{2}}}{30 b^{*2} N_1^2}\right] \\ &- \frac{\mathrm{Br}}{8b^{*2}}\left[-\frac{y^{*2}}{2} + \frac{\{1+4b^*(N_1 y^* + c_1)\}^{\frac{7}{2}}}{140 b^{*2} N_1^2} \right. \\ &+ \frac{\{1+4b^*(N_1 y^* + c_1)\}^{\frac{5}{2}}}{20 b^{*2} N_1^2} \\ &\left. - 3\left\{\frac{y^{*2}}{2} + 2b^* N_1 \frac{y^3}{3} + 2b^* c_1 y^{*2}\right\}\right] \\ &+ c_5 y^* + c_6 \end{aligned} \tag{39.3}$$

$$\begin{aligned} \theta_2^* = &-\frac{\mathrm{Br}}{4b^{*2}}\left[y^{*2} - 2b^* N_1 \frac{y^3}{3} - 2b^* c_3 y^{*2} \right. \\ &\left. - \frac{\{1-4b^*(N_1 y^* + c_3)\}^{\frac{5}{2}}}{30 b^{*2} N_1^2}\right] \\ &+ \frac{\mathrm{Br}}{8b^2}\left[\frac{y^{*2}}{2} - \frac{\{1-4b^*(N_1 y^* + c_3)\}^{\frac{7}{2}}}{140 b^{*2} N_1^2} \right. \\ &- \frac{\{1-4b^*(N_1 y^* + c_3)\}^{\frac{5}{2}}}{20 b^{*2} N_1^2} \\ &\left. + 3\left\{\frac{y^{*2}}{2} - 2b^* N_1 \frac{y^{*3}}{3} - 2b^* c_3 y^{*2}\right\}\right] \\ &+ c_7 y^* + c_8 \end{aligned} \tag{39.4}$$

Constants c_1, c_2, c_3, c_4, c_5, c_6, c_7 and c_8 are evaluated from the boundary conditions given by Eqs. (22.1)-Eq. (22.4).

6. Results and discussion

Results of the present study are useful in the polymer flow processing, food processing, etc. where the Brinkman number is large, such as in the range of 1-10 [17]. The polymer materials generally have thermal conductivity k in the range of 0.1-0.5 W/m-K [17], dynamic viscosity in the range of 10-1000 Pa.S [17]. Taking typical value of the reference velocity as 0.05-2 m/s [17]

and temperature difference in the range of 10-50°C [17], Brinkman number ranges from 0.1 to10, which is lower than values encountered in practical situations. Thermophysical properties of fluids such as thermal conductivity, specific heat vary with temperature. If this variation is not considered, Brinkman number estimated may be in the higher side. However, in practice, due to the variation of the properties with temperature, lower values are experienced. In the present study, range of Brinkman number has been considered in the range 0.1-5. Therefore, in the present study, Brinkman number has been varied in the range of 0.1-5. The Sisko fluid parameter has been varied in the range of 0.05-0.5. It is important to note that higher value of b^* represents a fluid with more features of a Sisko fluid. Where as relatively small values of b^* indicates smaller deviation from Newtonian behaviour. But in previous studies of Sisko fluids, researchers have assumed Sisko fluid parameter b^* in small range only. For example, in study of researchers (Khan *et al* [9]), b^* has been varied in the range 0-0.8. Following this, in the present study too, b^* has been assumed to vary in small range of 0.05-0.5. Another important factor for considering this range is limitation of the Homotopy Perturbation Method (HPM) employed for solving the non-linear governing equations. In HPM, though presence of any small parameter is not required, but results are accurate only for a limited range of parameters. Otherwise, for relatively large parameter, the results diverge and generates results with poor accuracy. Considering these factors, in the present study, b^* has been varied in the range 0.05-0.5.

From the solution procedure outlined above, variation of velocity, flow rate, temperature have been presented as functions of parameters like Sisko fluid parameter, pressure gradient, Brinkmann number, non-Newtonian index. The trend of the results has also been explained from the physics of the problem.

6.1 *Validation of the results*

Before, carrying out a study on parametric variation, first, results of the present study are validated. For validation purpose, results of the present study are compared with that of the numerical results generated by solving the governing equations by numerical technique. Equations (11)–(14) alongwith the boundary conditions given by Eqs. (19.1)–(19.4) are solved by employing shooting method. Equations are discreitized using finite difference scheme. A guess value for the slope of velocity is assumed and iterated till zero velocity is obtained at the upper wall. The convergence criteria for the velocity is considered as 10^{-6}. Once the velocity is obtained, then temperature distribution is generated using the velocity. Moreover, for validation purpose, exact solutions for velocity and temperature are obtained for the non-Newtonian index n=2. Figure 2 presents a comparison between the results obtained from HPM and numerical solution. Further, results generated by HPM for n=2, are compared with the exact solution. It is evident from figure 2 that the results are in excellent agreement which shows suitability of HPM for solving non-linear differential equations. This gives a confidence that HPM can yield analytical solutions for values of n other than 2, even if the infinite series is truncated after a few terms.

6.2 *Velocity distribution*

Velocity distribution for different values of the non-Newtonian index n, treating b^* as a parameter is presented in figure 3. For each n, three different values of b^* = 0.05, 0.25 and 0.45 are considered when N_1=-3. It is evident from the graph that with an increase in b^*, velocity decreases significantly in each case. As b^* increases, effective viscosity (Eq. (16)) increases. For a pressure-driven flow, an increase in the effective viscosity causes an increase in the flow resistance. This higher resistance causes a lower velocity for the pressure driven flow.Similar trend is observed in the results obtained by Khan *et al* [9]. From figure 3, it can be noted that when the Sisko fluid parameter b^* increases from 0.05 to 0.25, the maximum velocity decrease by nearly 11%.

From Eq. (6), it can be observed that a higher value of N_1 indicates higher pressure gradient or a lower value of the material constant a. Effect of non-dimensional pressure gradient N_1 on the velocity has been presented in figure 4. The results clearly represents that pressure gradient affects velocity significantly. With an increase in the non-dimensional pressure gradient, velocity increases. Higher pressure gradient causes higher velocity. Lower value of the material constant a, too, results in a lower effective viscosity causing a higher velocity. From figure 4, it can be noted that with an increase in N_1 from -1 to -2, the maximum velocity increases by nearly 83%. Effect of non-Newtonian index n on the velocity distributions is depicted in figure 5. The results indicate that the velocity increases with an increase in n. From Eq. (16), it is evident that with an increase in n, effective viscosity of the Sisko fluid decreases when velocity gradient is less than unity. In this case it can be shown that velocity gradient is less than unity in the considered range of parameters, which results in a decrease in effective viscosity. Therefore, velocity increases with the increase in n for pressure driven flow. However, this increase in velocity with n is less significant for higher values of n. In this regard, it is important to note that increase in velocity with an increase in n is not in violation of the characteristics of the shear-thickening fluids. It is known that for shear thickening fluids, effective viscosity increases with an increase in shear stress and the reverse happens for shear thickening fluids. In the present study, values of n are considered as 2, 3 and 4. The results

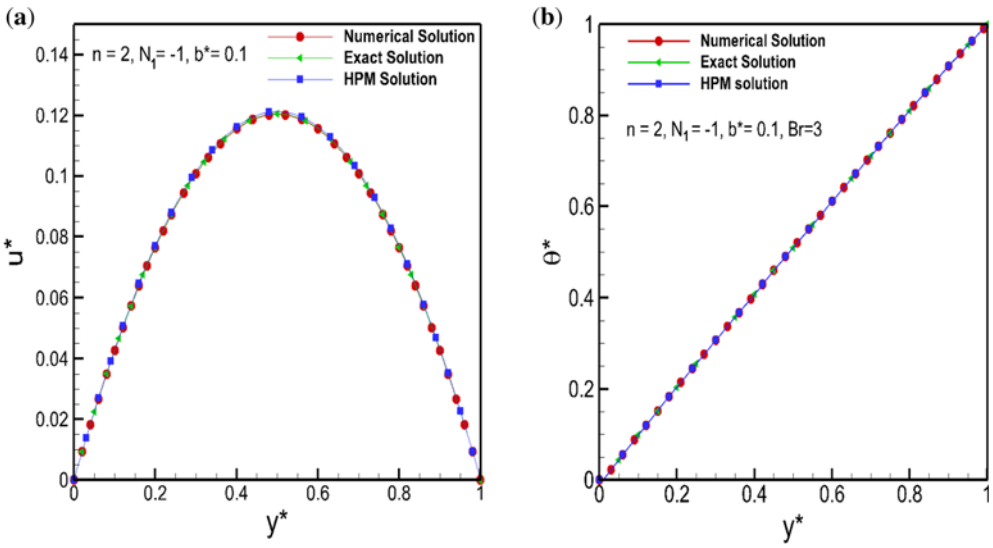

Figure 2. Non-dimensional (a) velocity and (b) temperature distributions from numerical, exact and HPM solution for $n = 2$ and $N_1 = -1$, Br = 3, $b^* = 0.1$.

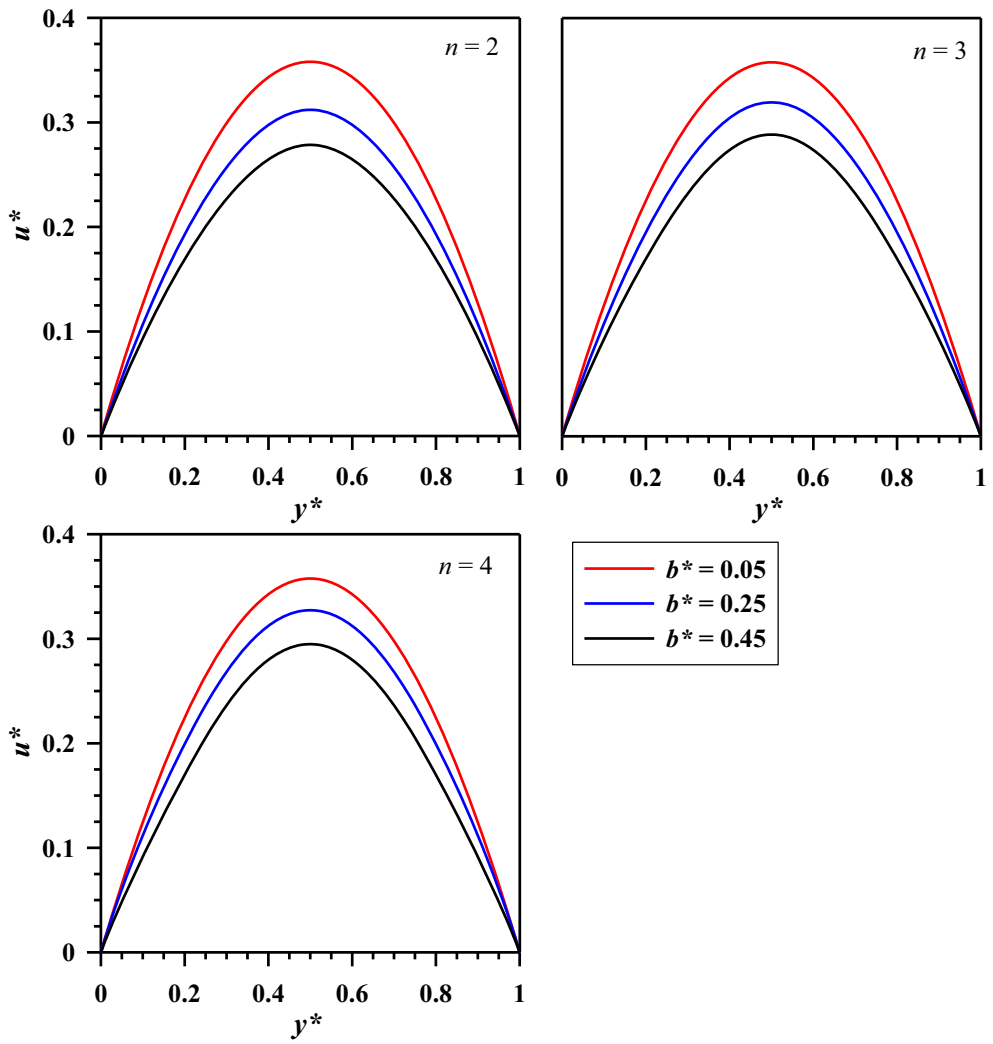

Figure 3. Non-dimensional velocity profile for different values of n and b^* for N_1=-3.

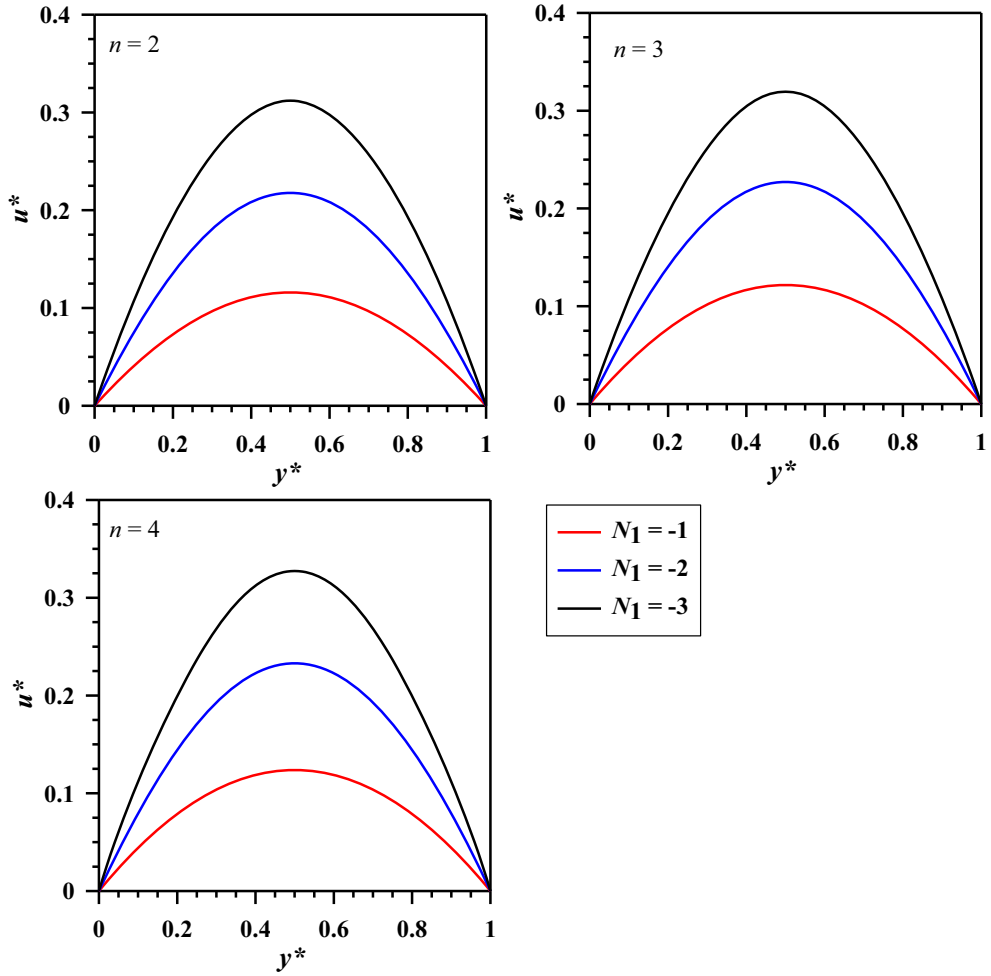

Figure 4. Dimensionless velocity profile in the channel for different values of n and N_1 for $b^* = 0.25$.

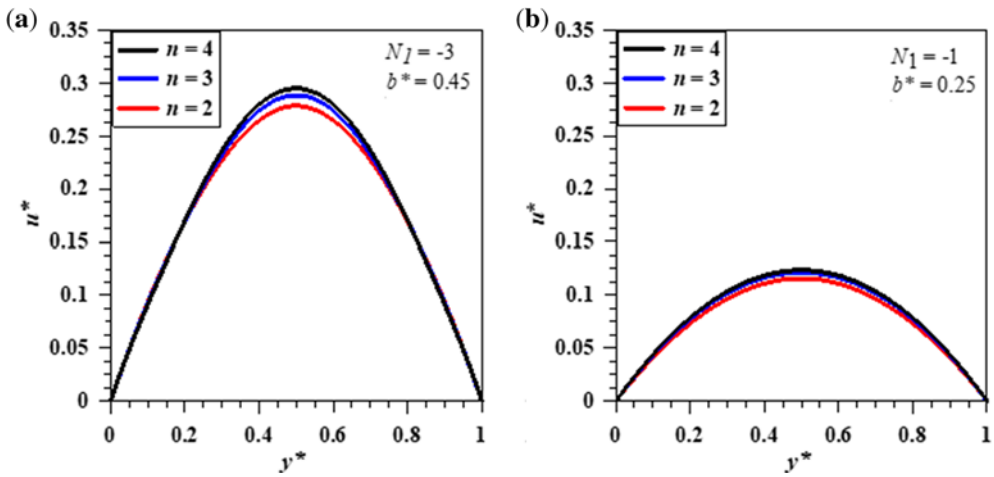

Figure 5. Dimensionless velocity profile along the channel for different values of n.

presented in figure 5 are valid for the case when fluid is subjected to same shear but at higher values of n. This does not represent the case of increasing the shear for a fixed value of n. Therefore, increase in the velocity with an increase in n is not in violation of the characteristics of shear thickening fluids (n>1).

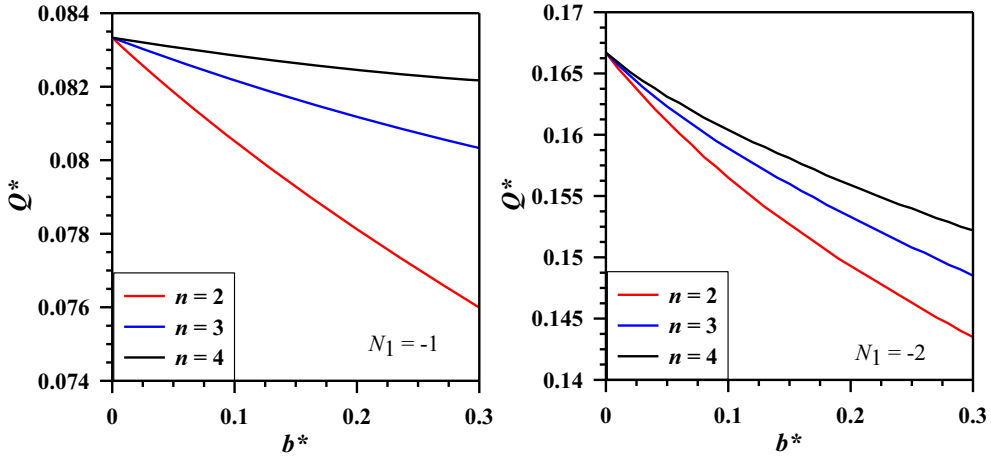

Figure 6. Dimensionless flow rate variation with b^* for different values of n.

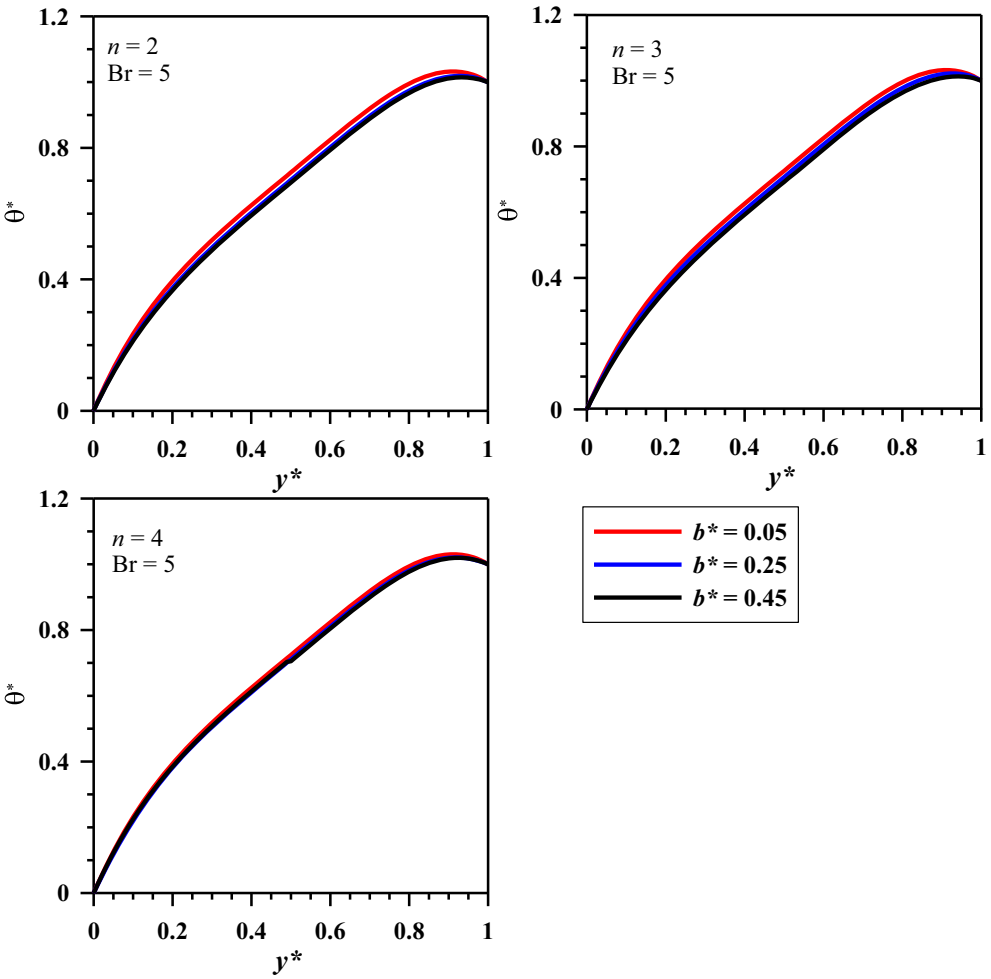

Figure 7. Dimensionless temperature profile in the channel for different values of n and b^*, $N_1 = -3$.

6.3 *Flowrate*

Figure 6 presents variation of flow rate with b^* for n=2, 3 and 4. It is evident from the figure that flow rate decreases with an increase in b^*. With an increase in b^*, velocity decreases as discussed earlier, resulting in a decrease in flow rate. It is to be noted that for b^* =0, for all values of the

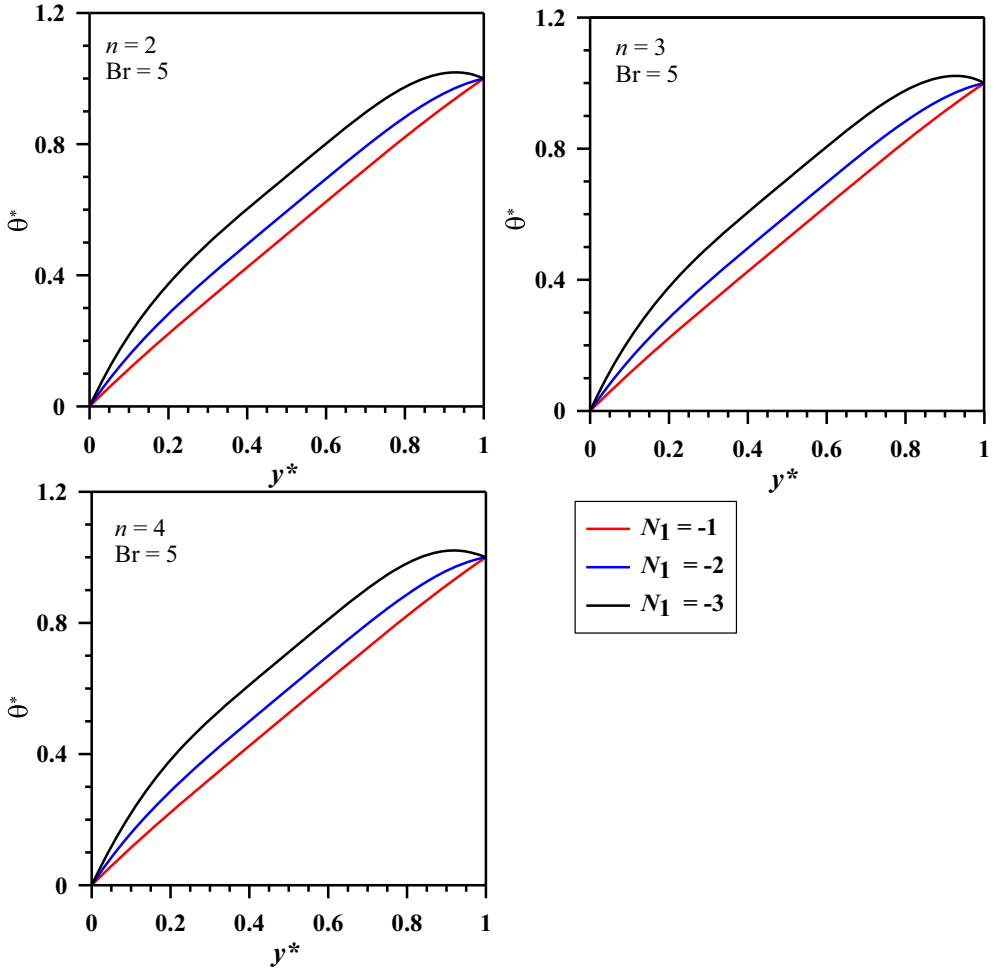

Figure 8. Dimensionless temperature profile in the channel for different values of n and N_1 for $b^* = 0.25$.

non-Newtonian index n, three graphs meet at a single point in the y axis, which indicates the non-dimensional flow rate for Newtonian fluid flow case. For the non-dimensional pressure gradient N_1=-1, the non-dimensional flow rate for b^*=0 is 0.0833 and for N_1=-2, it is 0.166. For other values of the Sisko fluid parameter b^* also, the flow rate is higher for N_1=-2 compared to the values at N_1=-1. Higher values of the flow rate are a result of higher pressure gradient.

6.4 *Temperature distribution*

Effect of b^* on the temperature distribution has been depicted in figure 7. The results indicate that with an increase in b^*, temperature decreases. However, this decrease in temperature is marginal which indicates that the effect of b^* on the the temperature is very little for the range of parameters considered. In the study of researchers (Khan *et al* [9]), Sisko fluid parameter has been considered in the range 0-0.8. Considering this in the present study, Sisko fluid parameter has been restricted in slightly lower range of 0.01-0.5. It has already been discussed that with an increase in b^*, velocity decreases at all points in the gap between the plates. As a result, velocity gradient (rate of change in velocity with respect to y) will be lower. It is well known that viscous dissipation effect is directly proportional to both velocity gradient and viscosity. For a lower velocity gradient, the effect of viscous dissipation will decrease even for higher values of b^*. Therefore, temperature decreases with an increase in b^*. It is important to note that the temperature reaches a maximum not at the upper wall but at a location close to it and its magnitude is nearly 5-10% higher than the upper wall temperature in each case. As the physical problem addressed in the present study is about the heat transfer through large parallel plates with a narrow gap, the effect of conduction heat transfer dominates over that of the heat transfer due to convection. It is already discussed that the combined effect of Peclet number and the ratio of the gap between the plates and axial reference length is less than unity ($h/l \ll 1$). Due to this factor, the effect of convection can be neglected and the heat transfer problem reduces to

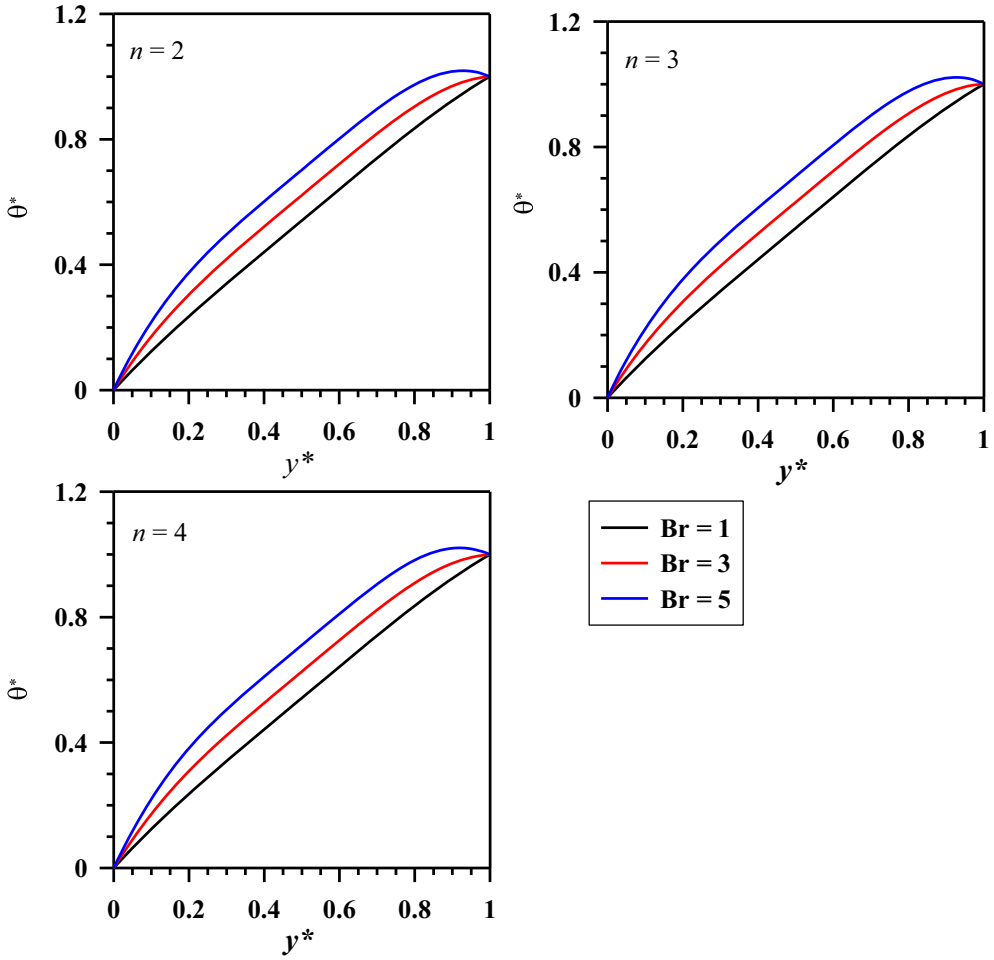

Figure 9. Dimensionless temperature profile for different values of n and Br for b^*= 0.25, N_1=-3.

an equivalent conduction problem. The temperature distribution, therefore, should follow a linear profile if the viscous dissipation effect is neglected. The non-dimensional temperature should be zero at the lower wall and following a linear profile it should reach unity at the upper wall. Non-linear nature of the distribution is attributed to the effect of viscous heating which acts an internal heat generating source. Figure 8 represents the effect of N_1 on the temperature distribution. The results clearly indicate that the pressure gradient has a significant effect on temperature distribution. With the increase in pressure gradient, velocity increases significantly as discussed earlier. With an increase in the velocity at all points, velocity near the plates also increases. Therefore, velocity gradient (du/dy) increases. Near the plates, this increases is higher. This higher velocity gradient causes a higher viscous dissipation which finally results in a higher temperature of the fluid. It is important to note that the fluid temperature reaches the peak within the range of 85-90% of the depth and its magnitude is nearly 10% higher than the upper wall temperature.

Effect of the Brinkman number on temperature distribution has been depicted in figure 9. It is evident from the figure that temperature increases significantly with an increase in Br. Higher values of Brinkman number signify higher viscous dissipation. This viscous dissipation acts as an internal heat generation source and results in an increase in temperature at all points in the fluid. In the absence of viscous dissipation, the temperature profile reduces to a straight line indicating a conduction problem without any internal heating source. For Br=1, the graphs clearly reveal that the temperature distribution follows almost a linear profile, implying that the deviation from the linear profile of conduction problem is marginal.When *Br=3*, temperature at all points, except neat the walls, increases by 25%. As *Br* increases from 3 to 5, peak temperature near the upper wall increases from 0.95 to 1.05 indicating 10% increase. In absence of viscous dissipation, heat will flow from the upper wall to the lower wall and heat has to be removed from the lower wall. While, heat has to be supplied to the upper wall at the same rate of heat rejection from the lower wall. But in presence of the viscous dissipation, as the temperature near the upper wall

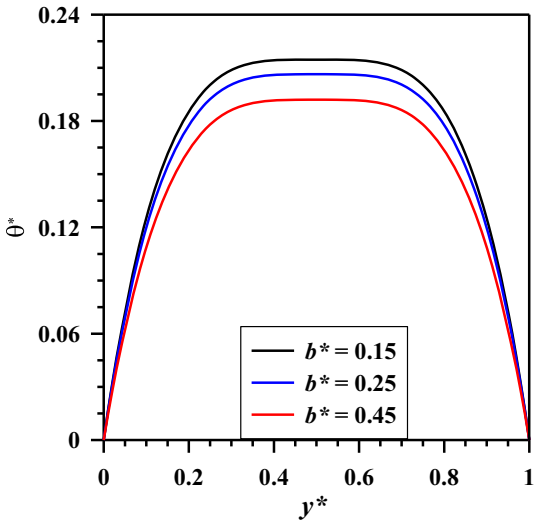

Figure 10. Dimensionless temperature distribution along the depth of the channel for same wall temperature for different values of $b^*$and n = 3 for Br= 5, N_1= − 3.

increases from that of the wall, heat will flow from the fluid to the wall and heat has to be removed from the upper wall. From the lower wall also, heat has to be removed but the rate of heat transfer will differ. That means in the presence of viscous dissipation, to keep the walls at constant temperature, heat has to carried away from both the walls and heat will flow from the fluid to both walls. It can be noted that with increase in *Br*, the peak value of the temperature, near the wall increases.

Figure 10 represents non-dimensional temperature distribution for n=3 along the depth of the plates for different values of b^* and same wall temperatures as a special case. These results represent the case when both the walls are maintained at same temperature. If both walls are maintained at same temperature, without the effect of viscous dissipation, there should not be any heat transfer through the fluid (convective heat transfer is neglected) and the temperature of the fluid will be same at all points. In presence pf the viscous dissipation, due to internal heating, temperature of the fluid increases at all points and due to symmetry temperature reaches the peak in the middle of the plates. Results imply that with an increase in the Sisko fluid parameter b, temperature decreases. With an increase in b^*, velocity decreases causing lower viscous dissipation. A considerable portion of the region between the parallel plates, has nearly the same temperature which is clear from the nearly flat temperature profile. This trend also indicates that with an increase in b^*, there is a significant temperature drop. This fact implies that with an increase in b^*, heat is to be transferred from the walls at a lower rate for maintaining the same wall temperatures. Due to symmetry, same quantity of heat is transferred from fluid to the walls and that heat is to be carried away by other means to maintain the constant temperature of the walls.

7. Conclusions

Pressure driven flow of a Sisko fluid through rectangular parallel plates with different wall temperatures has been investigated. Non-linear governing differential equations for the conservation of momentum and energy are solved using HPM and analytical solutions for velocity, flow rate, temperature are generated. Sisko fluid parameter, Brinkman number, non-dimensional pressure gradient have been varied widely to examine the effects of these variation on velocity, temperature. Following are the important observations made from this study:

- Velocity decreases with an increase in the Sisko fluid parameter significantly.
- Temperature decreases with an increase in the Sisko fluid parameter and the effect is marginal when the walls are maintained at different temperatures. But a significant effect on temperature is observed when both the walls are at the same temperature.
- Velocity increases with an increase in the non-Newtonian index for the considered range of parameters.
- Viscous dissipation effect is only significant when Br is higher than unity. Up to Br=1, the effect of conduction heat transfer dominates; beyond Br=1, effect of viscous dissipation,acting as an internal heat source, dominates and temperature distribution displays non-linear trend.
- Peak temperature is observed at nearly 90%-95% of the gap between the plates from the lower plate.

Results of the present study are useful for designing of thermal systems handling polymer flows and food items used in the food processing industries. In the present investigation properties are assumed to be temperature independent. For temperature dependent properties, governing equations turn out to be highly non-linear, which requires numerical techniques to be employed for solution. The analytical solution provided in the present study may serve useful for validating numerical results as no other previous analytical results are available in the literature.

Acknowledgement

The authors are thankful to the reviewers for their valuable and useful comments which have improved the quality of the manuscript.

References

[1] Tan W C and Xu M Y 2002 The impulsive motion of a flat plate in a generalized second order fluid. *Mech. Res. Commun.* 29(1):3–9

[2] Fetecau C and Fetecau C 2003 The first problem of Stokes for an Oldroid-B fluid. *Int. J. Nonlinear Mech.* 38(10):1539–1544

[3] Hayat T, Khan M, Ayub M and Siddiqui A M 2005 The unsteady Couette flow of a second grade fluid in a layer of porous medium. *Arch. Mech.* 57(5):405–416

[4] Qi, H T and Jin H 2006 Unsteady rotating flows of viscoelastic fluid with the fractional Maxwell model between coaxial cylinders. *Acta Mech. Sin.* 22(4):301–305

[5] Fetecau C, Fetecau C, Vieru D 2007 On some helical flows of Oldroyd-B fluid. *Acta Mech*. 189: 53–63

[6] Hayat T, Iqbal Z, Sajid M and Vajravelu K 2008 Heat transfer in pipe flow of a Johnson Segalman fluid. *Int. Commun. Heat Mass Trans.* 35(10):1297–1301

[7] Sisko A W 1958 The flow of lubricating greases. *Int. Eng. Chem*. 50:1789–1792

[8] Khan M S and Shahzad A 2012 On axisymmetric flow of Sisko fluids over a radially stretching sheet. *International Journal of Non-Linear Mechanics* 47: 999–1007

[9] Khan M, Munwar S and Abbasbandy S 2010 Steady flow and heat transfer of a Sisko fluid in annular pipe. *Int. J. Heat Mass Transf.* 53:1290–1297

[10] Siddiqui A M, Ahmed M and Ghori Q K 2007 Thin film flow of non-Newtonian fluids on a moving belt. *Chaos Solitons and Fractals* 3(33):1006–1016

[11] Khan M and Shahzad A 2013 On boundary layer flow of a Sisko fluid over a stretching sheet. *Questions Mathematicae* 36(1):137–151

[12] Bhatti M M, Zeeshan A and Ellahi R 2016 Endoscope analysis on peristaltic blood flow of Sisko fluid with Titanium magneto-nano particles. *Computers in Biology and Medicine* 78(1):29–41

[13] Shaheen A, Asjad, MI 2018 Peristaltic flow of a Sisko fluid over a convectively heated surface with viscous dissipation. *J. Phys. Chem. Solids* 122:210–217

[14] Zeeshan A, Ali N, Ahmed R, Waqus M and Khan W A 2019 A mathematical framework for peristaltic flow analysis of non-Newtonian Sisko fluid in an undulating porous curved channel with heat and mass transfer effect. *Computer Methods and Programs in Biomedicine* 182:105040

[15] Hayat T, Ullah I, Alsaedi A, Waqas M and Ahmed B 2017 Three-dimensional mixed convection flow of Sisko nano-fluid. *Int. J. Mech. Sci.* 133(273–282)

[16] Raja M A Z, Mehmood A, Rehman A ur, Khan A and Zameer A 2018 Bio-inspired computational heuristics for a Sisko fluid and heat transfer model. *Applied Soft Computing* 71(622–648)

[17] Gupta B R 2008 *Polymer Processing Technology* Asian Books Private Limited, New Delhi

[18] Khan Z, Khan A F, Islam S, Jan B, Hussain B, Rasheed H and Khan W 2017 Analysis of magneto-hydrodynamics flow and heat transfer of a visco elastic fluid through porous media in a wire coating analysis. *Mathematics* 5: 27

[19] He J H 1997 A new approach to nonlinear partial differential equations. *Commun Nonlinear Sci. Num. Simul.* 2(4):230–235

[20] He J H 2000 A coupling method of homotopy and perturbation technique for nonlinear problems. *Int. J. Non-linear Mech.* 35(1):37–43

[21] He JH 2003 Homotopy perturbation method, A new nonlinear analytic technique. *Appl. Math. Comput.* 135(1):73–79